JOURNAL OF CATALYSIS 66, 222–228 (1980)

Kinetics of Activated Chemisorption: Hydrogen on Scandium Oxide

J. L. GARCÍA FIERRO AND J. A. PAJARES

Instituto de Catálisis y Petroleoquímica del CSIC, Serrano 119, Madrid 6, Spain

Received February 27, 1980

The integral chemisorption kinetics of hydrogen on scandium oxide fits well the integrated Elovich equation. t_0 values from $Z(t)$ curves (Aharoni and Ungarish's method) agree with those obtained from q vs $\log(t + t_0)$ plots. The effects of pressure, temperature, and state of the surface have been studied. The adsorption is activated, with $E_a = 83 \pm 6$ kJ mol^{-1}, $Q = 67 \pm 5$ kJ mol^{-1} for $\theta = 0.37$. The remaining OH groups strongly influence both the initial rate and the adsorbed amount. Equilibrium adsorption follows the model of Freundlich.

INTRODUCTION

The Langmuir–Hinshelwood model assumes a rather idealized situation, in which the reaction proceeds on a homogeneous surface. Simple equations are obtained (*1, 2*), which fairly fit integral kinetic data in a wide interval of temperatures and pressure. However, many kinetic and equilibrium data of chemisorption, specially those of Taylor's school, show that most surfaces are heterogeneous: Q decreases, and E_a increases, with increasing θ. Kinetic data are often fitted to Elovich's equation (*3*), specially in the slower segments. Crickmore and Wojciechowski (*4*) claim for a consistent set of kinetic equations for adsorption and desorption, and, therefore, for the equilibrium situation.

Gundry and Tompkins (*5*) and Weinberg and co-workers (*6*) have pointed out that a precursor state leads to potential kinetic equations that lead, in the equilibrium, to Freundlich's isotherm (*4*). Following this line, Aharoni and Ungarish (*7*) assume a pre-Elovichian state to explain the failure of Elovich's equation to adequately describe the initial adsorption rate.

We have selected scandia as adsorbent, as it is a typical insulator oxide whose surface is relatively stable and easy to reproduce. The chemisorption kinetics of hydrogen and the influence of temperature, pressure, and hydroxylation of the adsorbent have been studied. Fitting of the results to an integrated Elovich equation has produced t_0 values in agreement with those calculated from $Z(t)$ curves (see below).

The H_2/Sc_2O_3 isobar corresponds to an activated system (*8*), with a maximum at about 648 K and two descending branches, one from 77 to 373 K, corresponding to a weak adsorption, and another one at temperatures higher than 648 K, corresponding to a moderately strong chemisorption. At these higher temperatures the isotherms correspond to type I of the BDDT system (*9*), and fit Freundlich's equation, with $Q = 68.1$ kJ mol^{-1} at $\theta = 0.37$. Q decreases exponentially with increasing θ, and the adsorption entropy is in excellent agreement with an immobile model. Infrared spectroscopy shows bands in the OH stretching region.

THE FUNCTION $Z(t)$

The differential Elovich equation is:

$$dq/dt = a \cdot e^{-bq} \qquad (1)$$

which gives on integration:

$$q = (1/b) \ln (ab) + (1/b) \ln (t + t_0), \qquad (2)$$

where q is the amount adsorbed at time t, and a, b, and t_0 are constants. If adsorption only obeys Eq. (1) from the beginning, then

0021-9517/80/110222-07$02.00/0

$q = 0$ at $t = 0$, and therefore:

$$t_0 = 1/(ab). \quad (3)$$

Equation (3) is rarely obeyed in practice. Therefore, a pre-Elovichian adsorption has been postulated (*10*), with the t_0 value that produces a linear q vs ln $(t + t_0)$ plot. This assumes that $q \neq 0$ at $t = 0$, which corresponds to:

$$t_0 = \frac{1}{ab} \cdot e^{bq_0}, \quad (4)$$

a t_0 value higher than that from Eq. (3), as b and q_0 are always ≥ 0.

Aharoni and Ungarish (*7*) have developed a simple method to obtain t_0 from experimental data without any assumption on the pre-Elovichian process. Equation (1) can be rewritten as:

$$t + t_0 = Z(t)/b, \quad (5)$$

where $Z(t) = (dq/dt)^{-1}$ is the reciprocal of the adsorption rate at time t. A plot of t vs $Z(t)$ will be linear in the Elovichian range, extrapolation to $Z(t) = 0$ directly giving t_0 as the intercept (Fig. 1).

EXPERIMENTAL

Materials

Sc_2O_3 p.a., 99.9%, with 0.03% of Y_2O_3 + Yb_2O_3 and traces of oxides of Si, Bi, and Pb as main impurities, was supplied by Fluka AG, Buchs, Switzerland. X-Ray diffraction confirmed its type C cubic structure. Electron microscopy and sedimentation gave a mean particle size of 2–4 μm. Scanning electron micrographs at 1500× and 5000× revealed great surface heterogeneity. Infrared spectra showed a band at 3665 cm^{-1} (*11*) of surface OH stretching vibration. Samples degassed above 873 K show another band of OH groups with a higher coordination, and with a coverage $= 0.3$ OH/nm^2 as determined by thermogravimetric analysis.

The samples were heated in air 4 hr at 973

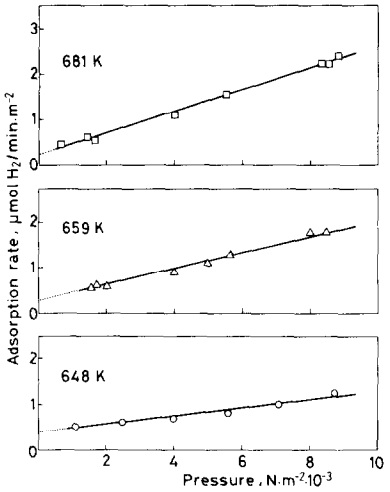

FIG. 2. Effect of pressure on initial adsorption rate: (□) 681 K; (△) 659 K; (○) 648 K.

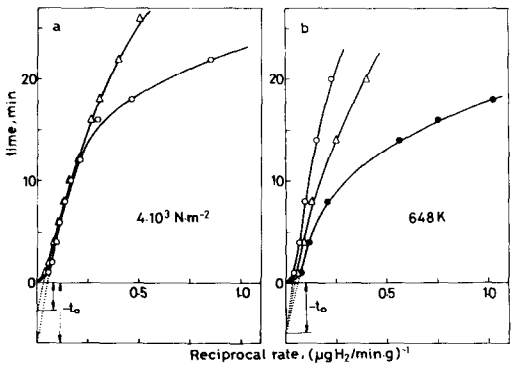

FIG. 1. Plot of t against Z. (a) Kinetic runs at 4×10^3 N m^{-2}: (○) 648 K and (△) 681 K. (b) Kinetic runs at 648 K: (○) 8.72×10^3; (△) 3.97×10^3; (●) 1.08×10^3 N m^{-2}.

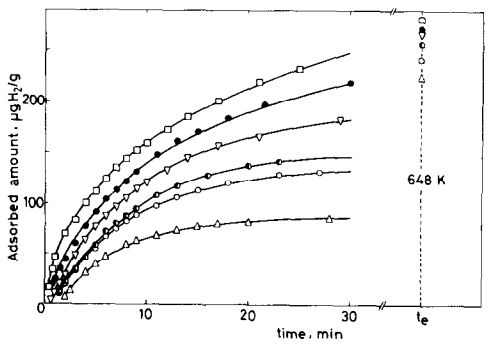

FIG. 3. Integral data at 648 K and different pressures: (□) 8.72×10^3; (●) 7.96×10^3; (▽) 5.56×10^3; (◐) 3.97×10^3; (○) 2.47×10^3; (△) 1.08×10^3 N m^{-2}.

K, after which they had a N_2 BET surface area of 12.6 m^2/g and a total macro- and mesopore volume of 0.06 cm^3/g. *t* curves point to a negligible micropore volume. N_2 adsorption–desorption isotherms show de Boer's type A hysteresis, typical of cylindrical or "ink bottle" pores (*12*). Heating to 973 K changes little the type of pore, but increases the size of micropores to mesopores (*13*).

H_2, 99.95%, was from SEO. It was passed through two series-connected U tubes with silica gel and active charcoal, respectively, immersed in an acetone–dry ice slush.

He, 99.995%, from SEO, was used for calibration. It was passed through the same system plus a trap in liquid N_2.

Apparatus and Procedures

An RG Cahn electrobalance connected to a conventional HV system was used (*11*). Its high dead volume (~4 dm^3) allows operation at constant pressure. Two coaxial furnaces in the sample- and the counterweight arms, respectively, minimize by symmetry the effect of the convention currents.

Both Sc_2O_3 powder ($d \leq 42$ μm) and coarse grains ($0.8 \leq d \leq 1.5$ mm) obtained by crushing low-pressure Sc_2O_3 pellets were used. Adsorption results were the same in the two cases, and therefore the last method was chosen in order to avoid sample dispersal during admission or removal of gases.

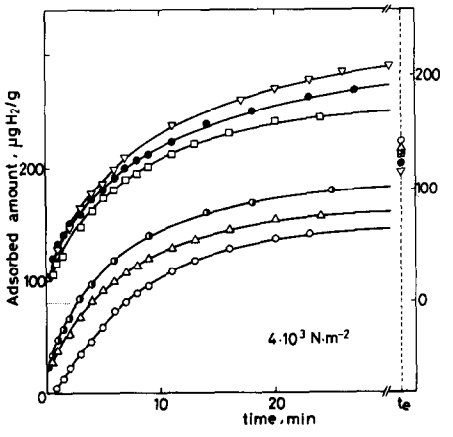

FIG. 4. Integral data at 4×10^3 N m^{-2} and different temperatures: (▽) 726 K; (●) 697 K; (□) 681 K; (◑) 673 K; (△) 659 K; (○) 648 K.

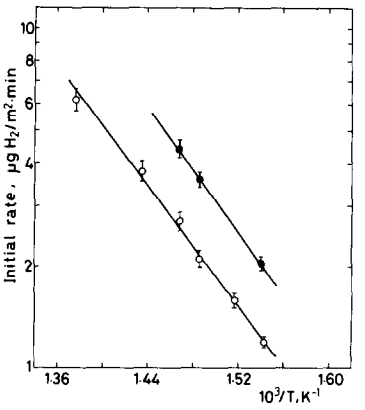

FIG. 5. Arrhenius plot of initial adsorption rates: (○) 4×10^3; (●) 8×10^3 N m^{-2}.

Samples (200–500 mg) were always degassed 16 hr at 1.33×10^{-4} N m^{-2} and 773 K. The thermomolecular effect was noticeable at pressures below 2×10^{-2} N m^{-2}, and may produce weight changes of 50–200 μg in the Knudsen region (5–0.1 N m^{-2}). To avoid this effect, 200–300 N m^{-2} He was introduced into the system after temperature equilibration. H_2 equilibrium pressure was determined to ±6.7 N m^{-2} by subtracting the He pressure from the total pressure. He admission produces a wave with an initial peak-to-peak amplitude of 10 μg, decreasing to 1–2 μg. The mean value was taken in all cases, and the equilibrium point was determined after Otto and Shelef (*14*).

Initial adsorption rates were obtained by analytical derivation after fitting the integral data for very short times to a hyperbolic function.

Samples were rehydroxylated *in situ* with 2×10^3 N m^{-2} H_2O for 50 hr at 323 K, after which they were degassed as above.

RESULTS

Effect of the Pressure

In Fig. 2 we represent the initial adsorp-

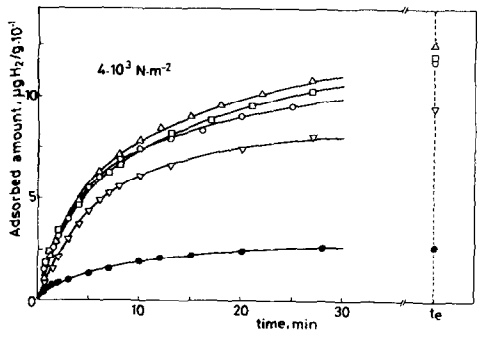

FIG. 6. Integral kinetic data at 429 K and 4×10^3 N m^{-2} for a sample dehydroxylated at different temperatures: (△) 770 K; (□) 562 K; (○) 501 K; (▽) 429 K. (●) Kinetic run at 323 K and 4×10^3 N m^{-2} for a sample dehydroxylated at 323 K.

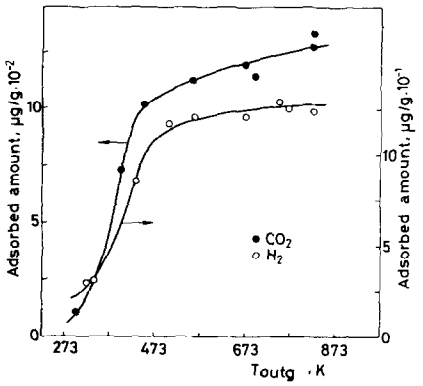

FIG. 7. Adsorbed amount at equilibrium vs outgassing temperature: (○) H_2 at 429 K and 4×10^3 N m^{-2}; (●) CO_2 at 296 K and 4×10^3 N m^{-2}.

tion rate as a function of adsorbate pressures ($50–10^4$ N m^{-2}) at 648, 659, and 681 K. The initial adsorption rate increases linearly with H_2 pressures at pressures higher than 10^2 N m^{-2}, although extrapolation produces a finite intercept. At pressures below 10^2 N m^{-2} the curve is slightly concave due to (i) thermomolecular effect (*15*) and (ii) control of the adsorption by diffusion in the gas phase.

Integral adsorption data at 648 K and several pressures in the range $5 \times 10^2–10^4$ N m^{-2} are given in Fig. 3. Also shown are the equilibrium adsorption obtained according to Otto and Shelef (*14*).

Effect of the Temperature

Integral kinetic curves for a constant pressure of 4×10^3 N m^{-2} and several temperatures in the range 648–726 K are given in Fig. 4. Also shown are the amounts adsorbed at equilibrium. These results are in complete agreement with those of González Tejuca *et al.* (*8*) for the H_2/Sc_2O_3 insobar in a wide temperature range.

An Arrhenius plot of the initial rates of adsorption at 4×10^3 and 8×10^3 N m^{-2}, respectively, is given in Fig. 5. The mean activation energy is 83 ± 6 kJ mol^{-1}, typical of an activated process.

As shown in Fig. 1, t_0 has been obtained by extrapolation to $Z(t) = 0$ of the linear segments of the t vs $Z(t)$ curves, following Aharoni and Ungarish's method (*7*).

Effect of the State of the Surface

The hydroxylation state of the surface influences both the initial adsorption rate and the amounts adsorbed at equilibrium (*2*). Integral kinetic data for 4×10^3 N m^{-2} and 429 K at several dehydroxylation temperatures in the range 429–770 K are given in Fig. 6. It can be seen that both the initial adsorption rate and the equilibrium adsorption decrease with decreasing temperature of outgassing. This effect was more clearly noticed on an experiment made over the sample outgassed at the same dehydroxyl-

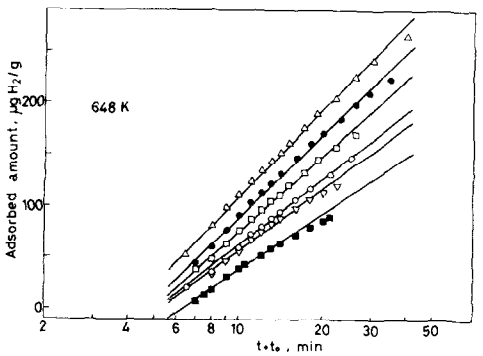

FIG. 8. Elovich plot for 648 K and different pressures: (△) 8.72×10^3; (●) 7.06×10^3; (□) 5.56×10^3; (○) 3.97×10^3; (▽) 2.47×10^3; (■) 1.08×10^3 N m^{-2}.

TABLE 1

Effect of Pressure: Parameters from Best Fit to Eq. (2)

P (N m^{-2} × 10^{-3})	a	b	$1/(ab)$ (min)	r (μmol/m^2 · min)
1.08	11.3	0.015	5.9	0.53
2.47	16.3	0.012	5.1	0.63
3.97	18.8	0.010	5.3	0.70
5.56	22.7	0.009	4.9	0.81
7.06	25.2	0.008_6	4.6	0.99
8.72	29.3	0.008	4.3	1.28

TABLE 2

Effect of Adsorption Temperature: Parameters from Best Fit to Eq. (2)

T (K)	a	b	$1/(ab)$ (min)	t_0[a] (min)
648	18.8	0.010	5.3	5.0
659	27.4	0.014	2.6	4.0
681	31.2	0.014_5	2.2	3.5
697	35.9	0.018	1.6	2.0
726	40.2	0.021	1.2	1.0

[a] Calculated from Eq. (5).

ation temperature (323 K) (solid circles in Fig. 6).

The equilibrium adsorbed amounts of 4 × 10^3 N m^{-2} H_2 and 4.25 × 10^3 N m^{-2} CO_2, respectively, for different dehydroxylation temperatures are plotted in Fig. 7 (*2, 16*). Both systems show similar behavior, with a marked decrease of H_2 adsorption for outgassing temperatures lower than 429 K, where OH coverage is greater than 2 OH/nm^2. This points to a competitive adsorption of H_2 and CO_2 with the OH groups on the surface (*2*).

DISCUSSION

Kinetic results were fitted to the integrated Elovich equation (2), although the classical differential equation (1) was used for the calculation of the kinetic adsorption constants.

Elovich plots for several pressures at 648 K are given in Fig. 8. Only one value of t_0 = 5 min was found in the whole range 1–9 × 10^3 N m^{-2} by extrapolation to $Z(t) = 0$ of the linear segments of t vs $Z(t)$ curves (*7*) (Fig. 1b). The corresponding values of a and b are given in Table 1. In the fourth column the values of $1/(ab)$ are also given; they are about 5 min, the same value calculated by Aharoni and Ungarish's procedure (*7*).

The initial adsorption rates at 648 K are given in the last column of Table 1. The linear increase of the initial adsorption rate with pressure (Fig. 2) obeys the reduction of Eq. (1) to its maximum value $dq/dt = a \propto p$ when $q = 0$. On this basis and assuming a Langmuir behavior, from the slopes in Fig. 2 the values of 1.5 ± 0.2 × 10^{-4}, 2.3 ± 0.2 × 10^{-4}, and 2.7 ± 0.2 × 10^{-4} N^{-1} m^2 min^{-1} for the kinetic adsorption constant at 648, 659,

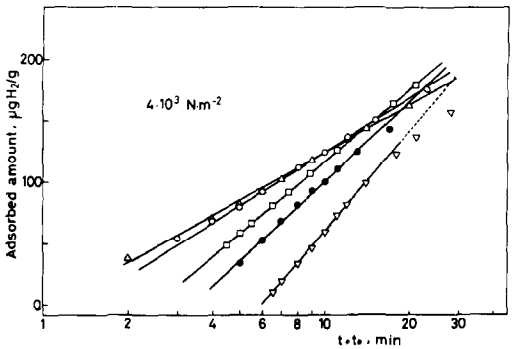

FIG. 9. Elovich plot for 4 × 10^3 N m^{-2} and different temperatures: (△) 726 K; (○) 697 K; (□) 681 K; (●) 659 K; (▽) 648 K.

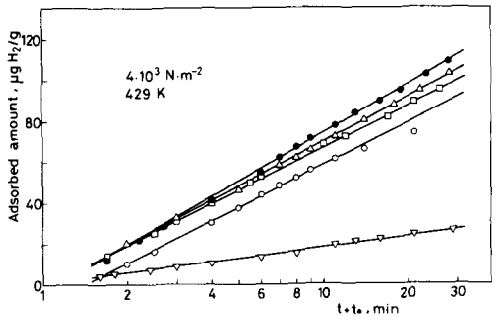

FIG. 10. Elovich plot for 429 K and 4 × 10^3 N m^{-2} of a sample dehydroxylated at different temperatures: (●) 770 K; (△) 562 K; (□) 501 K; (○) 429 K. (▽) Adsorption at 323 K and 4 × 10^3 N m^{-2} for a sample dehydroxylated at 323 K.

TABLE 3

Effect of the State of Hydroxylation of the Surface: Parameters from Best Fit to Eq. (2)

T_{outgas} (K)	T_{ad} (K)	a	b	$1/(ab)$ (min)	$r \times 10$ (μmol/m^2 · min)
323	323	0.05	0.128	0.37	2.30
429	429	6.07	0.037	1.30	3.93
501	429	27.3	0.036	1.01	6.84
562	429	31.0	0.033	0.98	8.10
770	429	33.8	0.029	1.02	9.45

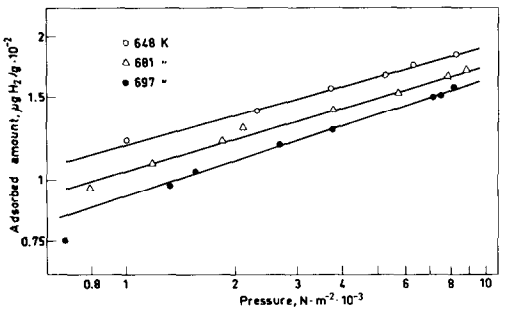

FIG. 11. Freundlich isotherms at different temperatures: (●) 697 K; (▽) 681 K; (○) 648 K.

and 681 K, respectively, have been calculated.

Elovich plots for 4×10^3 N m^{-2} and several temperatures in the range 648–726 K are given in Fig. 9. The corresponding t vs $Z(t)$ curves (Fig. 1a) show that in this case t_0 is a function of temperature, with a minimum value of 1 min at the highest temperature (726 K) and of 5 min for the lowest temperature (648 K).

The parameters a, b, and $1/(ab)$ and the value of t_0 obtained by Aharoni and Ungarish's method (*7*) are given in Table 2 for five temperatures. There is a fair agreement between $1/(ab)$ and t_0 from Aharoni and Ungarish's method, with the exception of the results for 659 and 681 K.

The high value of the apparent activation energy, 83 ± 6 kJ mol^{-1} (Fig. 5), is far lower than that of 130 kJ mol^{-1} found by Varadarajan and Viswanathan (*17*) for H_2 adsorption on a ZnO–MoO_3 catalyst. This is to be expected, as in the last case the adsorption is followed by a chemical reaction with a high activation energy. On the other hand, the adsorption of CO_2 on Sc_2O_3 is practically unactivated, with formation of surface carbonates.

Elovich plots for 4×10^3 N m^{-2} and 429 K for a sample outgassed at 429, 501, 562, and 770 K, respectively, are given in Fig. 10. Also given is an experiment with both outgassing and adsorption at 323 K. The calculated Elovich parameters and initial adsorption rates are given in Table 3. Outgassing temperature, i.e., remaining OH coverage, greatly influences adsorption. At the lowest outgassing and adsorption temperature, 323 K, the initial adsorption rate is fairly low and $1/(ab)$ is appreciably smaller than t_0 from Aharoni and Ungarish's method.

The influence of the remaining OH groups on the equilibrium adsorption is important for adsorption models. This influence has been reported by Pajares *et*

TABLE 4

Adsorbed Amounts of H_2 and CO_2 for Different Outgassing Temperatures

T (K)	n (OH/nm^2)	q_{H_2} (μg/g)	q_{CO_2} (μg/g)
373	6.2	47	460
423	4.3	78	805
473	2.7	105	1040
573	2.0	120	1150
673	1.4	125	1200
773	0.9	128	1250

TABLE 5

Parameters of Freundlich Isotherms for H_2 Adsorption on Scandium Oxide[a]

T (K)	n	nT (K)	$Q_m = nRT$ (kJ/mol)	$Q_m^{HT} = \frac{nRT}{1 - rT}$ (kJ/mol)	c (μg/g)
648	8.48	5495	45.7	67.6	163
681	7.97	5425	45.1	68.4	159
697	7.69	5360	44.5	68.4	144
			av Q_m = 68.1		

[a] $r = 0.53 \times 10^{-3}$ K^{-1}.

al. (*2*) for CO_2 on Sc_2O_3 and by Morimoto and Morishige (*18*) for CO_2 on ZnO, and has also been found here. The adsorbed equilibrium amounts of H_2 and CO_2 on Sc_2O_3 as a function of OH coverage are given in Table 4. The plot of equilibrium adsorption vs OH coverage is nearly a straight line with negative slope which points to a competition between OH and H_2 (or CO_2) for available surface sites.

Double-log Freundlich plots for three temperatures (648, 681, and 697 K) in the pressure range $(0.5–10) \times 10^3$ N m^{-2} are given in Fig. 11. A similar fit was found in a previous work with the same system (*8*), with adsorption heats decreasing with coverage, from 117 kJ mol^{-1} at $\theta = 5 \times 10^{-4}$ to 90 kJ mol^{-1} at $\theta = 0.05$.

The parameters n and c in Freundlich's equation,

$$q = c \cdot p^{1/n}, \qquad (6)$$

are given for the three temperatures in Table 5. The value $Q_m = nRT$ (adsorption heat at $\theta = 0.37$) is given in the fourth column. As Q_m decreases slightly with increasing T, the Halsey and Taylor value (*19*) $Q_m^{HT} = nRT/(1 - rT)$ with $r = 0.53 \times 10^{-3}$ K^{-1} is given in the fifth column. Q_m^{HT} is about 68 kJ mol^{-1}, in reasonable agreement with the already reported value (*8*) of 90 kJ mol^{-1} at $\theta = 0.05$ as the model predicts an exponential decrease of adsorption heat with increasing coverage.

ACKNOWLEDGMENT

We thank the Comisión Asesora para la Investigación Científica y Técnica for a grant.

REFERENCES

1. Ritchie, A. G., *J. Chem. Soc. Faraday Trans. I* **1,** 1650 (1977).
2. Pajares, J. A., García Fierro, J. L., and Weller, S. W., *J. Catal.* **52,** 521 (1978).
3. Low, M. J. D., *Chem. Rev.* **60,** 267 (1960).
4. Crickmore, P. J., and Wojciechowski, B. W., *J. Chem. Soc. Faraday Trans. I* **73,**1216 (1977).
5. Gundry, P. M., and Tompkins, F. C., *Trans. Faraday Soc.* **52,** 1609 (1956).
6. Weinberg, W. H., Comrie, C. M., and Lambert, R. M., *J. Catal.* **41,** 489 (1976).
7. Aharoni, C., and Ungarish, M., *J. Chem. Soc. Faraday Trans. I* **72,** 400 (1976); **73,** 456, 1943 (1977).
8. González Tejuca, L., Jandula, C., and García Fierro, J. L., *Z. Phys. Chem. (Frankfurt am Main)* **118,** 99 (1979).
9. Brunauer, S., Deming, L. S., Deming, W. E., and Teller, E., *J. Amer. Chem. Soc.* **62,** 1723 (1940).
10. Aharoni, C., and Tompkins, F. C., *Advan. Catal.* **21,** 1 (1970).
11. Pajares, J. A., González de Prado, J. E., García Fierro, J. L., González Tejuca, L., and Weller, S. W., *J. Catal.* **44,** 421 (1976).
12. De Boer, J. M., *in* "The Structure and Properties of Porous Materials" (D. H. Everett and F. S. Stone, Eds.), p. 68. Butterworths, London, 1958.
13. Mendioroz, S., García Fierro, J. L., and Pajares, J. A., unpublished results.
14. Otto, K., and Shelef, M., *J. Catal.* **14,** 226 (1969).
15. Loyalka, S. K., *J. Chem. Phys.* **66,** 4935 (1977).
16. García Fierro, J. A., and Pajares, J. A., *in* "Proceedings of the 5th Ibero-American Symposium on Catalysis" (P. Farinha and C. Pulido, Eds.), Vol. 1, p. 141, Lisboa, 1978.
17. Varadarajan, T. K., and Viswanathan, B., *Curr. Sci.* **48,** 17 (1979).
18. Morimoto, T., and Morishige, K., *Bull. Chem. Soc. Japan* **47,** 92 (1974).
19. Halsey, G. D., and Taylor, S. H., *J. Chem. Phys.* **15,** 624 (1947).